Transport in Porous Media **41:** 121–135, 2000.

An Analysis of the Movement of Wetting and Nonwetting Fluids in Homogeneous Porous Media

WEN-LU CHAO, J.-YVES PARLANGE* and TAMMO S. STEENHUIS
Department of Agricultural and Biological Engineering, Riley-Robb Hall, Cornell University, Ithaca, NY 14853, U.S.A.

(Received: 31 July 1998; in final form: 25 January 2000)

Abstract. The movement of wetting and nonwetting fluid flow in columns packed with glass beads is used to understand the more complicated flows in homogeneous porous media. The motion of two immiscible liquids (oil and water) is observed with different surfactants. Through dimensional analyses, fluid velocity is well correlated with interfacial tension and less dependent on particle size. In water–oil (W/O) experiments, finger pattern flows are observed if water is the displacing fluid that flows in an oil-filled porous media, whereas oil ganglia tend to form if oil is the displacing fluid in the water-wetted porous media. The results are well described by a simple model based on an earlier theory of flow in a tube.

Key words: wetting and nonwetting fluids, finger flow, interfacial tension.

1. Introduction

Past research on the movement of two fluids in closed tubes has focused mainly on the movement of a light fluid (gas) bubble rising through a more dense fluid (liquid) (Fabre and Liné, 1992). The propagation rate of a long gas bubble rising in a vertical closed tube has been investigated by several researchers (Dumitrescu, 1943; Davies and Taylor, 1950; Harmathy, 1960; Goldsmith and Mason, 1962; Zukoski, 1966; Tung and Parlange, 1976; Rimmer *et al.*, 1996). Zukoski (1966), in particular, described in detail the motion of long bubbles in closed tubes under the influence of viscosity, interfacial tension, and inclination angles, but did not focus on the wetting problem of two immiscible liquids.

Following the work of Powers *et al.* (1996) and Chevalier *et al.* (1997) the overall aim of this paper is to study experimentally and theoretically the movement of water, with surfactants, through oil in a soil to ultimately increase the efficiency of cleaning up oil spills. Related studies for improving oil recovery have been carried out in the past by Ng *et al.* (1978) and Payatakes and Dias (1984). Approaches in modeling multiphase systems for cleaning up soils have been reviewed recently in Miller *et al.* (1998). These experimental studies have concentrated on the study of oil ganglia and their recovery, whereas ours is more concerned with the penetration

* Corresponding author, e-mail: jp58@cornell.edu

of water and a soil saturated with oil. The understanding of flow in simulation models (or in analyzing experimental results) is usually based on the use of Darcy's law, that is, a continuum approach. Limited aspects of the flow are sometimes analyzed in a more fundamental way (e.g., Constantinides and Payatakes, 1991). The flow of water typically takes the form of narrow fingers involving few pores and the use of Darcy's law might be questionable. Instead, our approach is based on adapting an earlier theory of two-fluid flow in a closed tube (Tung and Parlange, 1976; Rimmer *et al.*, 1996). Rimmer *et al.* (1996), investigated the motion of two immiscible liquids (oil and water) in closed tubes without beads and found that the nonwetting liquid left smears on the tube wall and the wetting liquid moved erratically along the wall. This had a major effect on the flow characteristics. In this paper, the addition of beads makes the results more directly applicable to porous media. The specific objective of this paper is, therefore, to examine the influence of both the liquid properties and the size of the beads on the flow pattern. Experiments were performed with water and Soltrol 220 in cylindrical tubes (made either of glass or acrylic) using three different bead sizes. To examine the effect of interfacial tension, different surfactants were used in the water.

2. Materials and Methods

We performed two types of experiments: 'finger experiments' where a small amount of water (with or without surfactants) was initially at the top of the tube (made from either acrylic or glass) and then moved downwards as fingers, displacing oil that moved upwards. For completeness sake we also carried out some 'ganglia experiments' where a small amount of oil was, initially, at the bottom of the tube and then moved upwards a ganglia, displacing the water. An experimental summary is given in Table I.

The fluids used were distilled water and Soltrol 220 (a light oil that is a mixture of alkanes C_{13} through C_{17}). In order to enhance the contrast between these two fluids, either FD&C #1 (blue) and Sudan IV (red) were used in water and oil, respectively, in a concentration of 0.005%. In each experiment, the fluid initially present was transparent and the moving fluid was always colored. Thus, if water was the displacing fluid, the oil was clear and the water was blue, and if oil was the displacing fluid, the oil was red and the water was clear.

Two different types of tube materials, Pyrex glass and plastic (acrylic), with 2.5 cm inside diameter and 120 cm in length were used. The experimental setup is sketched in Figure 1. There were four different surfactant solutions (all 1% by weight) which can be classified into two groups: nonionic (Alfonic 810-4.5 Ethoxylate (Alphonic) and Surfynol 485 (Surfinol)), and anionic (Neodol R (Neodol) and Ploy Sodium Vinyl Sulfonate (PSVS)). The interfacial tensions between surfactant solutions and oil measured with a Fisher Surface Tensiomat Model 21 are listed in Table II. The viscosity of Soltrol was 3.64×10^{-2} g cm^{-1} s^{-1} (data supplied by Phillips 66 Company), while that of water was 1.005×10^{-2} g cm^{-1} s^{-1}.

Table I. The combinations of experiments in both the glass and acrylic tubes. The fingering experiments are those when displacing fluids are surfactant solutions; otherwise, they are ganglia experiments

Bead size (mm)	Tube material	Displacing fluid	Volume (ml)	Displaced fluid
4	Glass/acrylic	1% Neodol	22	Soltrol
4	Glass/acrylic	1% Alphonic	22	Soltrol
4	Glass/acrylic	1% Surfinol	22	Soltrol
4	Glass/acrylic	1% PSVS	22	Soltrol
4	Glass/acrylic	Water	22	Soltrol
3	Glass/acrylic	1% Neodol	22	Soltrol
3	Glass/acrylic	1% Alphonic	22	Soltrol
3	Glass/acrylic	1% Surfinol	22	Soltrol
3	Glass/acrylic	1% PSVS	22	Soltrol
2	Glass/acrylic	1% Neodol	22	Soltrol
2	Glass/acrylic	1% Alphonic	22	Soltrol
2	Glass/acrylic	1% Surfinol	22	Soltrol
2	Glass/acrylic	1% PSVS	22	Soltrol
4	Glass/acrylic	Soltrol	22	1% Neodol
4	Glass/acrylic	Soltrol	22	1% Alphonic
4	Glass/acrylic	Soltrol	22	1% Surfinol
4	Glass/acrylic	Soltrol	22	1% PSVS
4	Glass/acrylic	Soltrol	22	Water
3	Glass/acrylic	Soltrol	22	1% Neodol
3	Glass/acrylic	Soltrol	22	1% Alphonic
3	Glass/acrylic	Soltrol	22	1% Surfinol
3	Glass/acrylic	Soltrol	22	1% PSVS
2	Glass/acrylic	Soltrol	22	1% Neodol
2	Glass/acrylic	Soltrol	22	1% Alphonic
2	Glass/acrylic	Soltrol	22	1% Surfinol
2	Glass/acrylic	Soltrol	22	1% PSVS

In both the ganglia and finger experiments, 212 mm and 22 ml of water, respectively, was poured into the tube first. Beads were then added in 10 cm increments and tamped until there was no free-standing liquid remaining. This resulted in water-saturated beads of 108 and 12 cm for the ganglia and finger experiments, respectively. Oil was then added, followed by beads (in 10 cm increments) so that the top of the 120 column was filled with beads and saturated with oil. Three glass bead sizes (2, 3, and 4 mm in diameter) were used. The experiment was started by overturning the tube. Each experiment was repeated five times.

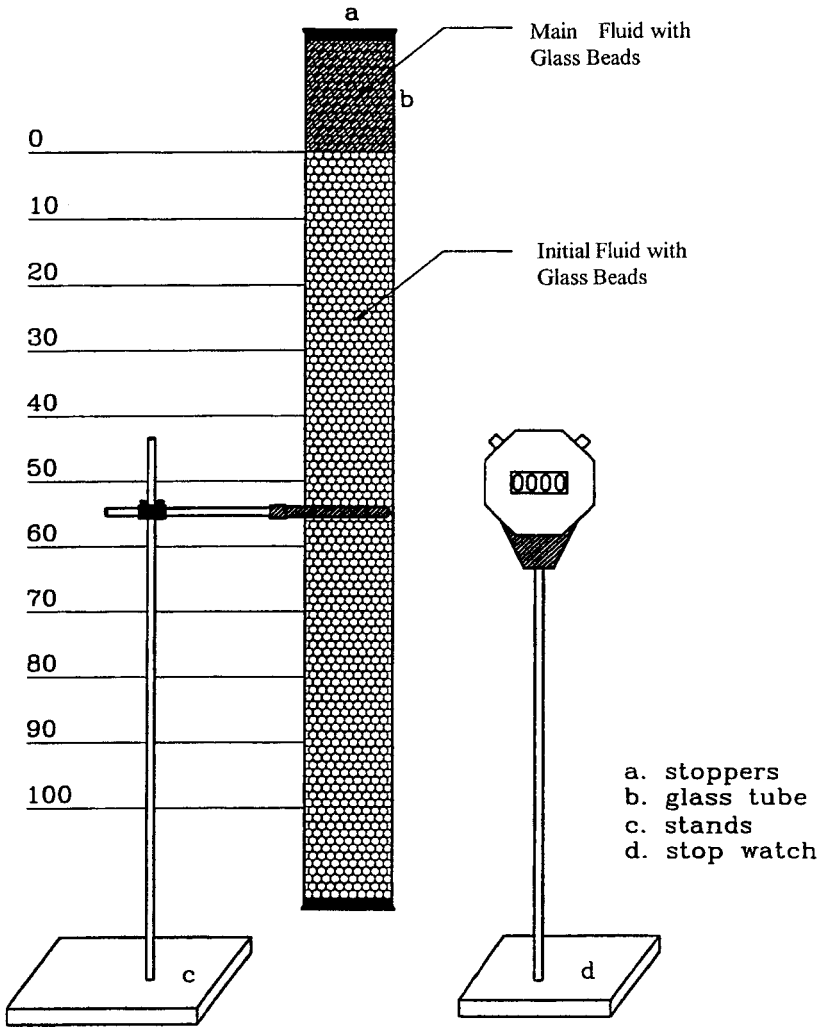

Figure 1. Experimental apparatus – glass or acrylic tube, glass beads with two immiscible fluids.

Table II. The interfacial tension ($g\,s^{-2}$) for 1% solvents of different solutions with Soltrol 220 oil

Water	Neodol	Alphonic	Surfinol	PSVS
32.8	1.9	5.9	11.4	28.6

Photographs were taken at times when the finger tips had advanced 20 cm. Both the flow pattern in the tube and a stopwatch to record the time were photographed (Figure 1). The finger velocity was determined from these pictures. The velocity of the first 20 cm was not considered because the exact time when the finger formation started was not recorded. Due to the difficulty of the ganglia to reach the top of tubes, velocities of ganglia were not determined. The width of the fingers was determined by counting the number of beads in a single finger. Ganglia were defined in a similar way.

3. Dimensional Analysis

There are nine variables and properties entering our experiment:

ρ_o = density of oil,
ρ_w = density of water,
μ_o = viscosity of oil,
μ_w = viscosity of water,
U = velocity of displacing fluid,
r = bead radius,
a = tube radius,
g = gravitational acceleration,
σ = interfacial tension of the two fluids.

Dimensional analysis gives six dimensionless numbers, for example,

$$\frac{\rho_w}{\rho_o}, \quad \frac{\mu_w}{\mu_o}, \quad \frac{r}{a}, \quad R^* = \frac{\Delta\rho^{2/3} g^{1/3} r}{\mu_w^{2/3}},$$
$$\sigma^* = \frac{\sigma\,\Delta\rho^{1/3}}{\mu_w^{4/3} g^{1/3}} \quad \text{and} \quad U^* = \frac{U\,\Delta\rho^{1/3}}{\mu_w^{1/3} g^{1/3}}. \tag{1}$$

The ratios of ρ_w/ρ_o and μ_w/μ_o do not vary in our experiments since we use the same fluids in all experiments. r/a is very small and irrelevant as the flow is controlled by the glass bead size and not by tube diameter. R^* is the dimensionless radius, σ^* is the dimensionless interfacial tension, and U^* is the dimensionless velocity. It is noted that the displacing fluid turns out to be water, the wetting fluid in fingering experiments when significant motion takes place. We use $\Delta\rho$, the density difference of the fluids, in the functions of R^*, σ^*, and U^* as the motion is caused by this difference. We want to investigate the relationship between U^*, σ^*, and R^* for fingers.

It is worth noting that the three numbers R^*, σ^*, and U^* are not the 'usual' numbers in immiscible displacement experiments such as the Froude (Fr), Reynold's (Re), Bond (Bo), and capillary (Ca) numbers. Of course they are related, for example,

$$\mathrm{Fr} = \frac{U^{*2}}{R^{*2}}, \qquad \mathrm{Re} = U^* R^*, \qquad \mathrm{Bo} = \frac{\mathrm{Re}^{*2}}{\sigma}, \qquad \mathrm{Ca} = \frac{U^*}{\sigma^*}. \tag{2}$$

The use of R^*, σ^*, and U^* is dictated here by the fact that in each of the three numbers only one variable appears: r, σ, and U, respectively, and the other parameters are constant in our experiments.

4. Results

In the 'ganglia' experiments (where the 22 ml of oil was at the bottom), the oil moved only upward in the 3 and 4 mm beads filled with the surfactant solutions. Small ganglia (1–2 mm) were formed with the resident solutions with the lowest interfacial tension consisting either of Neodol or Alphonic. Ganglia of 6–7 mm developed for the Surfinol and PSVS resident solutions (Table IIIa).

The 'finger' experiment flow patterns are shown in Figure 2 and are tabulated in Table IIIb. In general, the higher the interfacial tension the smaller the number of fingers: Neodol with a interfacial tension of 2 dyn cm^{-1} had up to 10 very small (1–2 mm) water fingers and Alphonic had an average of 4–5 (0.5 cm wide). In both cases, these fingers sometimes merged and formed larger fingers. Surfinol and PSVS had only 1 or 2 fingers while, for distilled water with the highest interfacial tension, the fingers did not form in the 2 and 3 mm beads.

After the tube was turned over, different amounts of time were needed for the instability to develop. For Neodol, Alphonic, and Surfinol, finger formation was almost immediate for all bead sizes. PSVS finger development was from 1 h

Table IIIa. The average sizes and predicted values of ganglia in 4, 3, and 2 mm glass beads with different surfactants

Bead size (mm)	Tube material	Surfactants (1%)	Flow patterns	Average size (mm)	Predicted width (mm)
4	Glass/acrylic	Neodol	Small ganglia	1.5	1.3
4	Glass/acrylic	Alphonic	Small ganglia	1.5	2.3
4	Glass/acrylic	Surfinol	Large ganglia	7.0	3.2
4	Glass/acrylic	PSVS	Large ganglia	7.0	5.0
3	Glass/acrylic	Neodol	Small ganglia	1.1	1.3
3	Glass/acrylic	Alphonic	Small ganglia	1.1	2.3
3	Glass/acrylic	Surfinol	Large ganglia	6.0	3.2
3	Glass/acrylic	PSVS	Large ganglia	6.0	5.0
2	Glass/acrylic	Neodol	Small ganglia	1.0	1.3
2	Glass/acrylic	Alphonic	Small ganglia	1.0	2.3
2	Glass/acrylic	Surfinol	Large ganglia	–	3.2
2	Glass/acrylic	PSVS	Large ganglia	–	5.0

The predicted values are obtained from Equation (3).

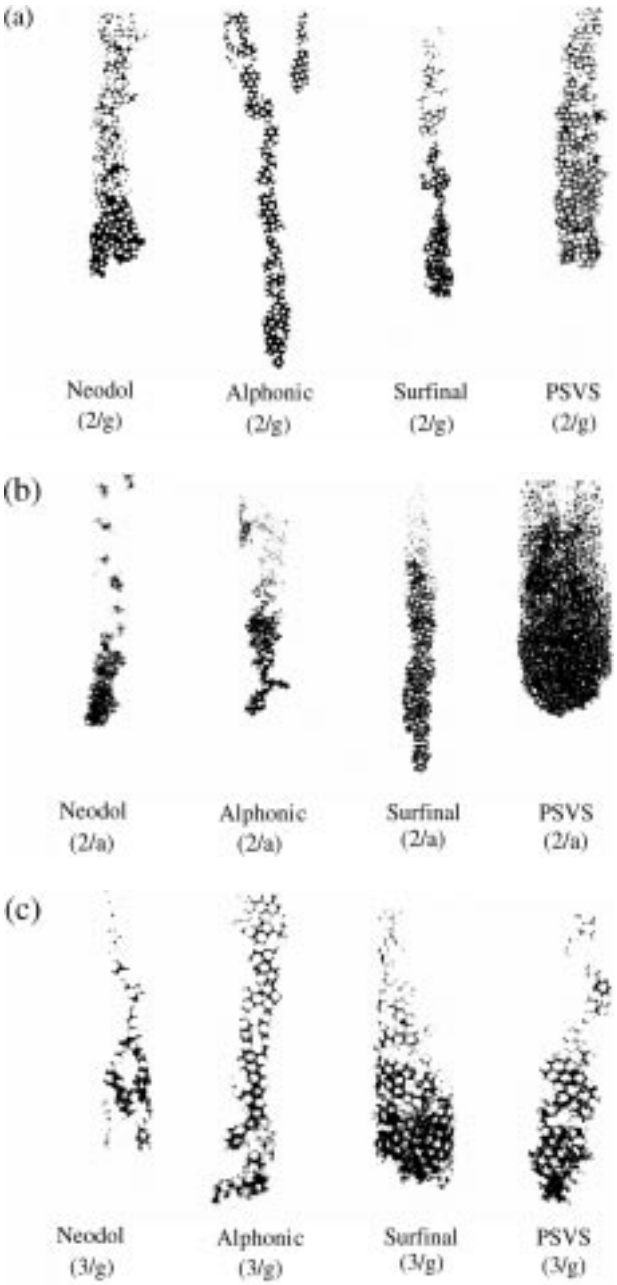

Figure 2. The finger flow patterns for the 'finger experiments', where 22 ml of water or surfactant solutions was initially ponded on top of Soltrol 220 in a tube filled with 2, 3, and 4 mm beads. The numbers in the parentheses indicate the bead sizes (mm) and the abbreviation of 'g' means glass tubes and 'a' means acrylic tubes.

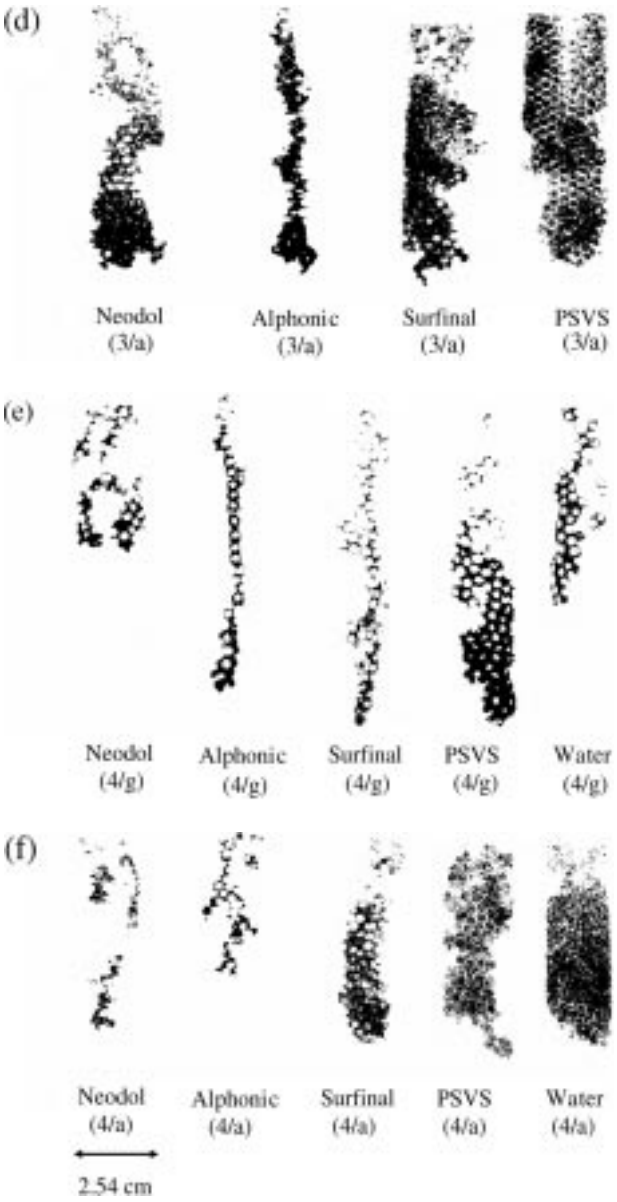

Figure 2. (Continued)

to 1 day. Finger development for water (without surfactant) took the longest time. For the 4-mm beads, initiation of finger formation was different between replications and it took anywhere from two to seven days. For the 2 and 3 mm beads, this period was in excess of a week. Once the instability was developed, the finger velocity increased, in general, with the interfacial tension except for PSVS which had a lower velocity than the Surfinol (Table IV). For the same surfactant,

Table IIIb. The number of fingers, average width and predicted width (Equation (3)) in 4, 3, and 2 mm glass beads with different surfactants

Bead size (mm)	Tube material	Surfactants (1%)	Number of fingers	Average width (mm)	Predicted width (mm)
4	Glass	Neodol	4-6	$\leqslant 2$	1.3
4	Glass	Alphonic	3–5	2	2.3
4	Glass	Surfinol	1–2	2–3	3.2
4	Glass	PSVS	1–2	4–6	5.0
4	Glass	None	1–3	4–6	5.4
4	Acrylic	Neodol	4–5	$\leqslant 2$	1.3
4	Acrylic	Alphonic	3–4	2.3	
4	Acrylic	Surfinol	1–2	2–3	3.2
4	Acrylic	PSVS	1	4–6	5.0
4	Acrylic	None	1–2	4–6	5.4
3	Glass	Neodol	10	1.5	1.3
3	Glass	Alphonic	5–7	1.5	2.3
3	Glass	Surfinol	2–3	1.5–3	3.2
3	Glass	PSVS	1	3–5	5.0
3	Acrylic	Neodol	8–10	1.5	1.3
3	Acrylic	Alphonic	3–4	2	2.3
3	Acrylic	Surfinol	1–2	3	3.2
3	Acrylic	PSVS	1–2	3–5	5.0
2	Glass	Neodol	>10	1	1.3
2	Glass	Alphonic	4–5	2	2.3
2	Glass	Surfinol	1–2	3	3.2
2	Glass	PSVS	1–2	4–5	5.0
2	Acrylic	Neodol	8	1	1.3
2	Acrylic	Alphonic	4–5	2	2.3
2	Acrylic	Surfinol	2–3	3	3.2
2	Acrylic	PSVS	1–2	6–7	5.0

the velocity in the glass tube was higher than in the acrylic tube. In the glass tube (which is hydrophilic), the finger moved along the walls and for the acrylic tube (extremely hydrophobic), the fingers traveled through the beads away from the wall.

5. Discussion

Rimmer *et al*. (1996) and Tung and Parlange (1976) give the Froude number as a function of interfacial tension in a tube, and we speculate that we can use this

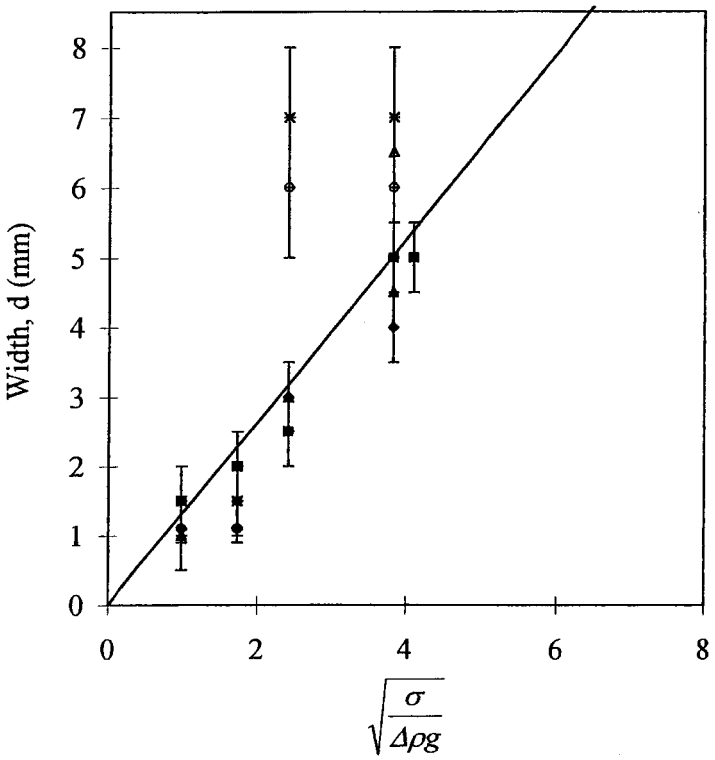

Figure 3. The linear relationship between finger widths and the sizes of ganglia with $\sqrt{\sigma/\Delta\rho g}$. The correlation coefficient (R) is 0.93. The solid line is the model obtained from Equation (3). The solid symbols (■, ★, and ▲) represent the glass tubes for 4, 3, and 2 mm, respectively. The open symbols (□, ◊, △) represent the acrylic tubes for 4, 3, and 2 mm, respectively. The star (⋆) is for large ganglia in 4 mm beads, while the open circle (○) is the large ganglia in 3 mm beads. The cross (×), solid circle (•), and plus (+) symbols represent small ganglia in 4, 3, and 2 mm beads, respectively.

equation because the presence of beads has the primary effect of increasing the resistance to flow. This equation applies and provides a relation between σ and the width of the finger, when no motion takes place, as

$$\frac{d}{2} = \left(\frac{0.472}{0.272}\right)^{1/2} \sqrt{\frac{\sigma}{\Delta\rho g}}. \tag{3}$$

Equation (3) suggests a linear dependence between the averaged width, d, and sqrt $\sqrt{\sigma/\Delta pg}$. This relationship has a correlation coefficient (R) of 0.93, and is well within the scatter of the data, as shown in Figure 3. Tables IIIa and IIIb also list predicted widths for ganglia and fingers following the regression relationship. We found that the widths of fingers and sizes of ganglia are primarily correlated with interfacial tension forces, rather than bead size, except possibly for larger sizes as found by Powers *et al*. (1991, 1992, 1994a, b).

Table IV. A detailed list of bead radius (r), averaged finger's wetting front velocity with standard deviations (U), interfacial tensions (σ) corresponding to different surfactants mentioned in Table II and also all the dimensionless numbers in finger experiments: $U^* = U\,\Delta\rho^{1/3}/\mu_w^{1/3}g^{1/3}$, $R^* = \Delta\rho^{2/3}g^{1/3}r/\mu_w^{2/3}$, and $\sigma^* = \sigma\,\Delta\rho^{1/3}/\mu_w^{4/3}g^{1/3}$

Tube	r (cm)	U (cm s^{-1})	σ (dyn cm^{-1})	U^*	R^*	σ^*	$\sigma^*/(R^*)^2$
Glass	0.20	0.39 ± 0.15	1.94	0.11	14.6	53.20	0.25
Glass	0.20	0.70 ± 0.32	5.91	0.19	14.6	159.6	0.75
Glass	0.20	0.28 ± 0.20	11.43	0.35	14.6	310.8	1.46
Glass	0.20	1.53 ± 0.26	28.62	0.42	14.6	776.9	3.64
Glass	0.20	1.23 ± 0.13	32.84	0.35	14.6	891.8	4.18
Acrylic	0.20	0.37 ± 0.15	1.94	0.10	14.6	53.20	0.25
Acrylic	0.20	0.69 ± 0.07	5.91	0.19	14.6	159.6	0.75
Acrylic	0.20	1.03 ± 0.10	11.43	0.28	14.6	310.8	1.46
Acrylic	0.20	0.58 ± 0.07	28.62	0.16	14.6	776.9	3.64
Acrylic	0.20	0.55 ± 0.05	32.84	0.15	14.6	891.8	4.18
Glass	0.15	0.35 ± 0.05	1.94	0.10	10.9	52.7	0.44
Glass	0.15	0.64 ± 0.15	5.91	0.18	10.9	160.4	1.35
Glass	0.15	1.16 ± 0.07	11.43	0.32	10.9	310.0	2.61
Glass	0.15	1.39 ± 0.42	28.62	0.38	10.9	776.9	6.54
Acrylic	0.15	0.36 ± 0.16	1.94	0.10	10.9	52.7	0.44
Acrylic	0.15	0.64 ± 0.05	5.91	0.17	10.9	160.4	1.35
Acrylic	0.15	0.88 ± 0.09	11.43	0.24	10.9	310.0	2.61
Acrylic	0.15	0.57 ± 0.07	28.62	0.15	10.9	776.9	6.54
Glass	0.10	0.28 ± 0.09	1.94	0.08	7.3	52.7	0.99
Glass	0.10	0.38 ± 0.14	5.91	0.10	7.3	160.7	3.02
Glass	0.10	0.41 ± 0.06	11.43	0.11	7.3	310.2	5.82
Glass	0.10	0.58 ± 0.21	28.62	0.16	7.3	776.8	14.6
Acrylic	0.10	0.22 ± 0.04	1.94	0.06	7.3	52.7	0.99
Acrylic	0.10	0.29 ± 0.03	5.91	0.08	7.3	160.7	3.02
Acrylic	0.10	0.56 ± 0.02	11.43	0.15	7.3	310.2	5.82
Acrylic	0.10	0.14 ± 0.02	28.62	0.04	7.3	776.8	14.6

Table IV shows that the velocities in the glass tubes were slightly higher than in the acrylic tubes. This was caused by the fact that for glass tubes, for which the walls were wettable, the fingers moved along the walls, while for hydrophobic acrylic tubes the fingers avoided the walls. Because the pore spaces are larger along the walls, the fingers in glass tubes moved presumably faster. However, during the immiscible displacements, emulsions sometimes appeared consisting of one liquid dispersed in another in the form of tiny droplets, with eventual separation of the phases (Becher, 1965; Clint, 1992). This separation of phases can be 20–30 cm

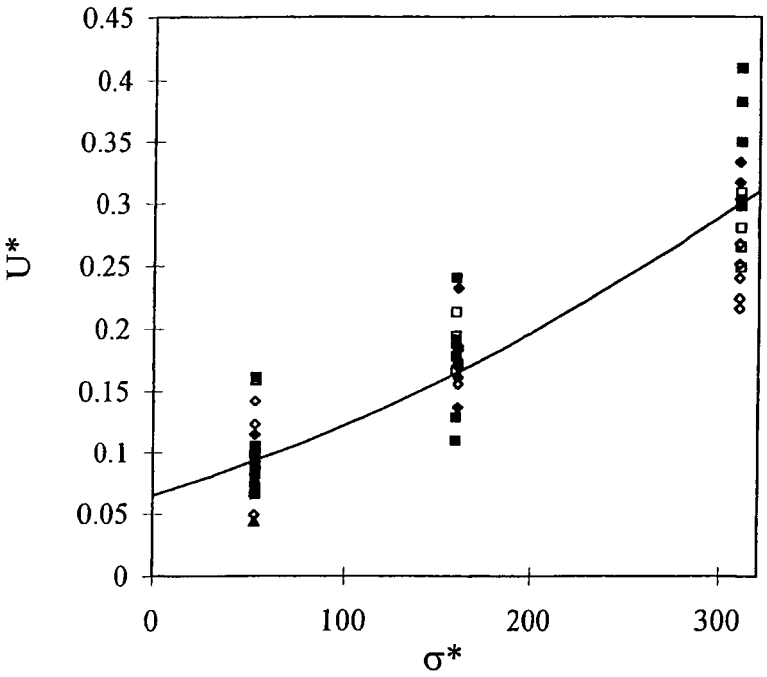

Figure 4. The curve line between U^* and σ^* in the glass and acrylic tubes with different beads when σ^*/R^{*2} is less than 3. The error of the glass tubes is 0.0498 while that of the acrylic tubes is 0.0407. The solid symbols (■, ★, and ▲) represent the glass tubes for 4, 3, and 2 mm, respectively. The open symbols (□, ◊, △) represent the acrylic tubes for 4, 3, and 2 mm, respectively.

long and reduce the fluid velocity dramatically when fluid flows into this region. It causes problems in determining the fluid velocity and observation of fluid motion in some emulsion-prone surfactants, such as Neodol and Alphonic, and it is most pronounced in the 2-mm beads in the glass tubes.

The dimensionless radius (R^*), interfacial tension parameter (σ^*), velocity (U^*), and ratio $\sigma^*/R^{*2}(\equiv 1/\mathrm{Bo})$ are also listed in Table IV. The fluid velocity, U^*, appears to be primarily a function of σ^*, and not bead size, r, as long as either σ^* is less or equal to 311 or σ^*/R^{*2} is less than 3 (i.e., Bond number greater than 3). For this range, as shown in Figure 4, a linear relationship of $\sqrt{U^*}$ and σ^* exists for both the glass and acrylic tubes with a correlation coefficient (R) of 0.921:

$$\sqrt{U^*} = 0.255 + 0.000941\sigma^*, \qquad \sigma^* \leqslant 311. \tag{4}$$

The error associated with the experimental data is obtained by

$$\text{error} = \frac{\sqrt{\Sigma(Y_i - \overline{Y}_i)^2}}{n}, \tag{5}$$

where residual $Y_i - \overline{Y}_i$ is the difference between the observed Y_i and the predicted $\overline{Y}_i$ with n degrees of freedom. Based on Equations (4) and (5), we obtain a relative

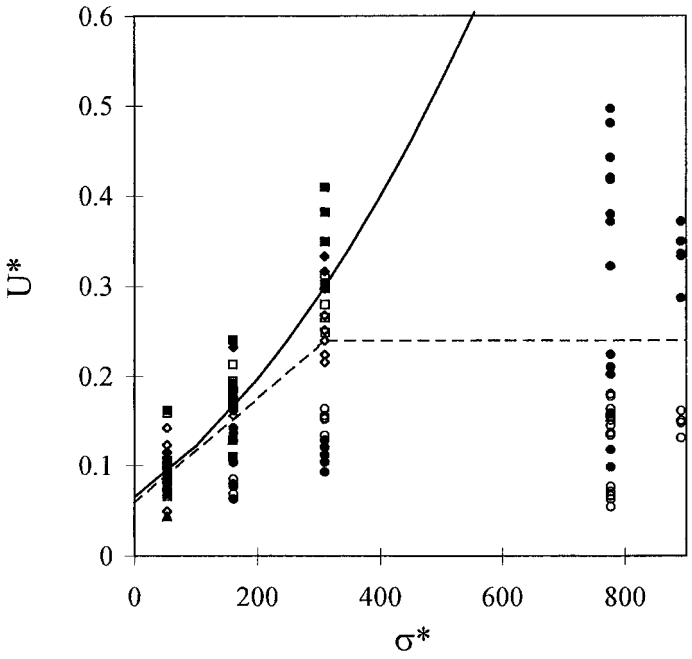

Figure 5. The data trends with σ/R^{*2} less than 3 (solid line) and all the data sets (dashed line). The relative error for all data sets is 0.0874. The solid bullet (•) represents the glass tubes, while the blank circle (○) represents the acrylic tubes. The separation of these two lines when σ^* is less than 311 caused by the contribution of the lower velocities cases when their σ^*/R^{*2} are larger than 3.

error of 0.0498 and 0.0407 for glass and acrylic tubes, respectively, which indicates the excellent agreement for both cases (Figure 4).

With the increase of σ^* above 311, more scatter data are always observed. In Figure 5, the velocities when σ^*/R^{*2} is greater than 3 ($\sigma^* > 310$), tend to be constant with very large scatter. Flow velocities in glass and acrylic tubes with σ^*/R^{*2} larger than 3 are lower than those with smaller σ^*/R^{*2} because of even smaller pores which enhance the difficulty for fluid displacements. Flows without surfactants tend to have lower velocities, presumably because of the contact angle problems. In Figure 5, which is the same as Figure 4 but with all σ^* values shown, there, obviously, exists two trends. The dashed line (all data) in Figure 5 gives us a linear relationship for σ^* less than 311, and a constant relationship for σ^* larger than 311:

$$U^* = 0.054 + 0.000583\sigma^*, \quad \sigma^* < 311, \tag{6a}$$

$$U^* = 0.24, \quad \sigma^* > 311. \tag{6b}$$

The relative error for all data trend is 0.0874 based on Equation (5). The result tells us that the flow velocity reaches a constant value if the interfacial tension is large

enough. Note that there is only a small difference in Figure 5 between the solid line (Equation (4)) and the dashed line (Equation (6)) as long as $\sigma^* \leqslant 200$. Also, note the very large scatter in the data in Figure 5 which is partly caused by the wetting (open circles), or nonwetting properties (solid circles) of the tube wall.

6. Conclusions

The displacement mechanism of two immiscible fluids (Soltrol 220 and water) in simple cylindrical tubes (glass and acrylic) filled with various glass bead sizes was studied to examine the influence of surfactants in the water. Tubes with 22 ml of displacement fluids at either the bottom or top (depending on if the displacement fluid was heavier or lighter than the residual fluid) were turned and flow patterns and sizes were documented. More thinner fingers and smaller ganglia were formed with the low interfacial tension surfactant (Neodol and Alphonic) solutions; whereas wider fingers and larger ganglia were present in high interfacial tension surfactant solutions (Surfinol and PSVS). The sizes of fingers and/or ganglia were found to be a function of interfacial tension, independent of particle sizes, and could be described by a relationship developed by Tung and Parlange (1976), and Rimmer *et al.* (1996). Within the scatter of the data, the dimensionless velocity (U^*) increases with the dimensionless interfacial tension parameter (σ^*) as long as σ^*/R^{*2} is less than 3 and is more or less constant if greater than 3.

References

Becher, P.: 1965, *Emulsions: Theory and Practice*, 2nd edn, Reinhold Pub., NY.

Chevalier, L. R., Masten, S. J., Wallace, R. B. and Wiggert, D. C.: 1997, Experimental investigation of surfactant-enhanced dissolution of residual NAPL in saturated soil, *Ground Water Monitoring and Remediation* **17**, 89–98.

Clint, J. H.: 1992, *Surfactant Aggregation*, Chapman and Hall, NY.

Constantinides, G. N. and Payatakes, A. C.: 1991, A theoretical model of collision and coalescnce of ganglia in porous media, *J. Colloid Interface Sci.* **141**, 486–504.

Davies, R. M. and Taylor, G. I.: 1950, The mechanics of large bubbles rising through extended liquids and through liquids in tubes, *Proc. Roy. Soc. London* **200A**, 375–390.

Dumitrescu, D. T.: 1943, Strömung an einer luftblase in senkrechten rohr. *Z. Angew. Math. Mech.* **23**, 139–149.

Fabre, J. and Liné, A.: 1992, Modeling of two-phase slug flow, *Annu. Rev. Fluid Mech.* **24**, 21–46.

Goldsmith, H. L. and Mason, S. G.: 1962, The motion of single large bubbles in closed vertical tubes, *J. Fluid Mech.* **14**, 42–58.

Harmathy, T. Z.: 1960, Velocity of large drops and bubbles in media of infinite or restricted extent, *AICHE J.* **6**, 281–288.

Miller, C. T., Christakos, G., Imhoff, P. T., McBride, J. F., Pedit, J. A. and Trangenstein, J. A.: 1998, Multiphase flow and transport modeling in heterogeneous porous media: challenges and approaches, *Adv. Water Resour.* **21**, 77–120.

Ng, K. M., Davis, H. T. and Scriven, L. E.: 1978, Visualization of blob mechanics in flow through porous media, *Chem. Engng Sci.* **33**, 1009–1017.

Payatakes, A. C. and Dias, M. M.: 1984, Immiscible microdisplacement and ganglion dynamics in porous media, *Rev. Chem. Engng* **2**, 85–174.

Powers, S. E., Loureiro, C. O., Abriola, L. M. and Weber, J. W., Jr.: 1991, Theoretical study of the significance of nonequilibrium dissolution of nonaqueous phase liquids in subsurface systems, *Water Resour. Res.* **27**, 463–477.

Powers, S. E., Abriola, L. M. and Weber, J. W., Jr.: 1992, An experimental investigation of nonaqueous phase liquid dissolution in saturated subsurface systems: Steady state mass transfer rates, *Water Resour. Res.* **28**, 2691–2705.

Powers, S. E., Abriola, L. M. and Weber, J. W., Jr.: 1994a, An experimental investigation of nonaqueous phase liquid dissolution in saturated subsurface systems: Transient mass transfer rates, *Water Resour. Res.* **30**, 321–332.

Powers, S. E., Abriola, L. M., Dunkin, J. S. and Weber, J. W., Jr.: 1994b, Phenomenological models for transient NAPL-water mass-transfer processes, *J. Contam. Hydrol.* **16**, 1–33.

Powers, S. E., Anckner, W. H. and Seacord, T. F.: 1996, Wettability of NAPL-contaminated sands, *ASCE J. Environ. Engng* **122**, 889–896.

Rimmer, A., Parlange, J.-Y. and Steenhuis, T. S.: 1996, Wetting and nonwetting fluid displacement in porous media, *Transport in Porous Media* **25**, 205–215.

Tung, K. W. and Parlange, J.-Y.: 1976, Note on the motion of long bubbles in closed tubes – Influence of surface tension, *Acta Mech.* **24**, 313–317.

Zukoski, E. E.: 1966, Influence of viscosity, surface tension and inclination angle on motion of long bubbles in closed tubes, *J. Fluid Mech.* **20**, 821–837.